

A Compact Solid State Transformer for Replacing Conventional Medium Power Transformer in Weight-Critical Applications

Leon Fauth, Felix Willer, and Jens Friebe

Institute for Drive Systems and Power Electronics - Leibniz University Hannover

Welfengarten 1

Hannover, Germany

Phone: +49 (0) 511-762-14571

Email: Leon.Fauth@ial.uni-hannover.de

URL: <https://www.ial.uni-hannover.de/en/>

Keywords

«Solid-State Transformer», «Resonant converter», «Gallium Nitride (GaN)»

Abstract

In certain weight-sensitive applications requiring galvanic isolation, conventional transformers can be of disadvantage due to their high weight and volume. Solid state transformers allow to overcome this issue. The volume can be further reduced by eliminating large dc storage capacitors, resulting in a straight AC/AC converter system based on a resonance converter.

Introduction

The operation of electrical equipment often requires galvanic isolation to the grid voltage for safety reasons, like in industrial grids or aircraft and marine applications. Conventionally, transformers are used, because of their well-proven design, robustness, and simplicity. However, in specific applications, tight requirements on volume, weight, or other parameters can exist, like for example in aircraft applications. Because of the usual grid frequency of 50 or 60 Hz, conventional transformers need a large active core cross sectional area and a high number of turns to avoid saturation. This leads to an overall high volume and weight. Also, conventional transformers allow for no controllability or intelligence. As an alternative, so-called solid state transformers (SST) can fulfil the same task. A SST will consist of a rectification block, a resonance converter, and an output inverter. If the operation frequency of the resonance tank is chosen sufficiently high, the volume of the magnetic components can be drastically reduced [1]. For a well-executed design, the system efficiency can be higher compared to conventional transformers. Also, the application of power electronics allows for a controllability during operation, for example to stabilize the output voltage amplitude. As design challenges, the higher component count and complexity has to be stated. If these issues can be solved during the design process, solid state transformers can be a good alternative for special applications. This paper shows the design of an ultra-compact SST. Also, the possibility to eliminate large DC storage capacitors is highlighted and the resulting waveforms and consequences on the control are shown [2]. The SST is designed as a direct replacement for a currently available off-the-shelf transformer. The reference off-the-shelf design has an overall volume of $150 \times 143 \times 113 \text{ mm}^3 = 2.42 \text{ L}$ and a weight of 7.9kg. The rated power is 630VA, the maximum efficiency is given as 93%. Isolation between primary and secondary side is rated as 5kV. It allows the transformation of various input voltage levels to a fixed output voltage by different winding taps. As an extension of the current state of research, the SST in this paper is designed for input voltages up to $U_{\text{in}} = 400 \text{ V}$, which results from a direct connection between two lines in a three-phase system, if no neutral line is available. Regardless of the input voltage, it will be converted to a stable output voltage of 230V by adapting the

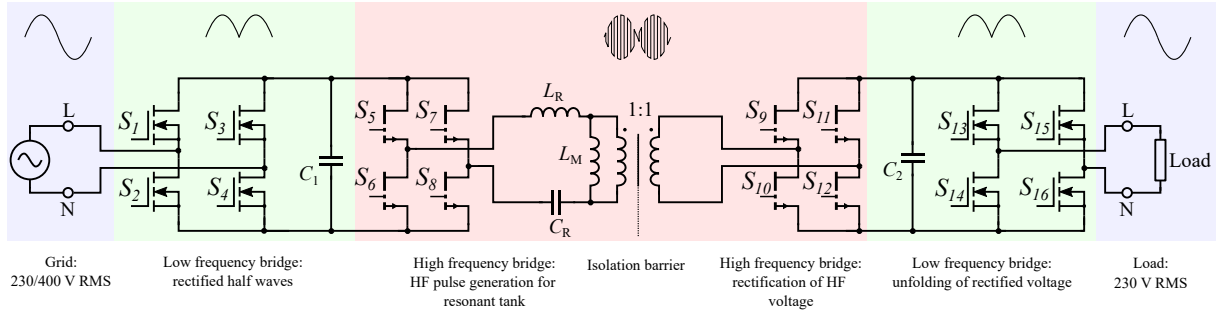


Fig. 1: Circuit diagram of the proposed system. All power electronics stages are used symmetrically on the primary and secondary side.

switching frequency of the resonance converter. For this operation, the resonance tank needs to be designed to allow for a sufficient minimum power level. Also, the compact realization of the hardware is highlighted with an integrated resonance inductor and transformer for the resonance converter.

Description of Topology

The chosen topology for the replacement solution is shown in Fig. 1. It consists of a fullbridge for input voltage rectification, the resonance converter, an output rectification and a fullbridge for unfolding the rectified voltage to a sine wave. The input fullbridge will rectify the grid voltage. To allow for reactive power capability, the switches S_1 to S_4 need to be active switches, for active power conversion, diodes can be used, but will typically result in higher losses. As the switching frequency is the same as the grid frequency, switching losses can be neglected, which allows the selection of power semiconductors with low conduction losses at lower cost. In this example, super junction MOSFETs optimized for a low channel resistance are selected. As stated before, for a pure AC to AC application, the capacitor C_1 can have a very low capacitance. If for example $C_1 = 1 \mu\text{F}$ is chosen, the capacitor voltage consists of sinusoidal half waves following the grid voltage. The capacitor is only used as a high frequency buffer for the following resonant converter. The resonant stage is designed as a series resonance converter (SRC) or a LLC-converter depending on the ratio of leakage and magnetizing inductance. A fullbridge (switches S_5 to S_8) is operated at a high switching frequency with 50% duty cycle. By that, a pulsed voltage with a sinusoidal envelope is generated over the resonance tank. The resonance frequency will be in the range of several hundreds of kilohertz, to allow for small magnetic components. As the resonance converter shall be operated at or above resonance to allow soft on-switching of the power semiconductors, gallium nitride switches with low switching energy are chosen. The transformer has to be designed for the high frequency components. Also, the required isolation level needs to be provided. In this case, 5 kV are selected based on the reference design. The high-frequency fullbridge consisting of the switches S_9 to S_{12} is used to rectify the output voltage of the resonant converter. A low capacitance value is used for C_2 . The resulting voltage is again consisting of sinusoidal half waves. Similar to the input fullbridge, diodes can be used if only active power needs to be transferred, but will result in higher conduction losses. For reactive power conversion, active switches are used, which need to be synchronized to the switching of the resonance converter fullbridge. Finally, the sinusoidal output voltage is generated by unfolding by the switches S_{13} to S_{16} . In summary, this leads to a fully symmetrical layout as shown in Fig. 1. Furthermore, under ideal conditions the switching signals from the primary side can also be used for the high- and low-frequency fullbridge on the secondary side. During the experimental tests it needs to be verified that even under real conditions, like non-ideal behaviour of gate drivers and propagation delay, a direct use of the primary side switching signals is possible.

Design of the Resonance Tank

The design strategy for the AC to AC resonance converter is shown in Fig. 2 and will be explained in the following. The design of the resonance tank, especially the magnetic components, holds several challenges. While designing the resonance elements L_R and C_R , the operation point for reducing the

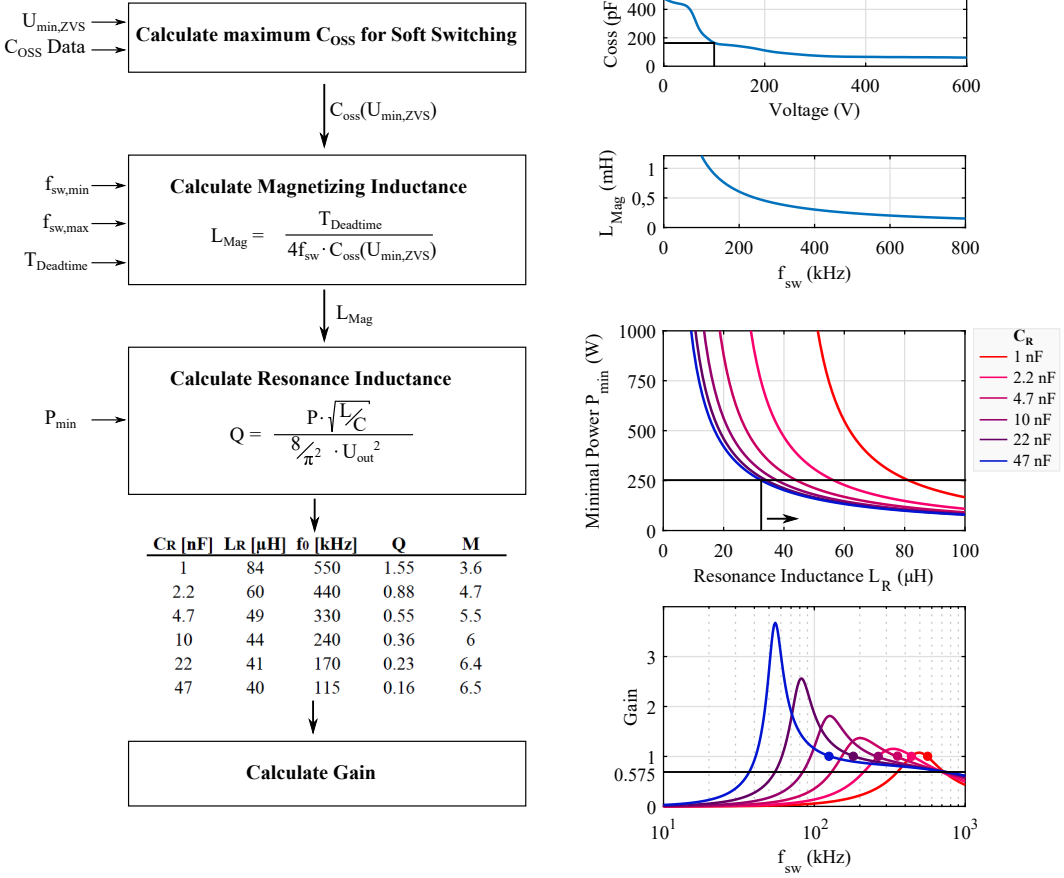


Fig. 2: Calculation of the resonance tank elements. From top to bottom: 1) Fixing of voltage threshold for soft switching for sinusoidal input voltages. 2) Dependency of maximum magnetizing inductance on the switching frequency. 3) Selection of resonance tank elements based on a minimal power for a gain of 0.575. 4) Resulting gain curves for different feasible combinations.

input voltage of $U_{\text{in}} = 400 \text{ V}$ to an output voltage of $U_{\text{out}} = 230 \text{ V}$ can mean restrictions on the minimum power. Therefore, careful consideration of chosen resonance frequency, inductance and capacitance value is necessary. Other challenges are due to the sinusoidal input voltage of the resonance converter, which influences the design of the magnetizing inductance of the transformer, affecting the operation area for soft on-switching.

For the conventional DC to DC operation of a resonant converter, the magnetizing inductance L_M can be designed to guarantee soft on-switching of the power semiconductors. For the here proposed AC to AC structure, certain trade-offs need to be made, as the input voltage of the resonance converter and therefore the blocking voltage of the power semiconductors are time-dependent. For low voltages, a very small magnetizing inductance value would be necessary to provide a sufficiently high magnetizing current for soft on-switching. This could result in an unreasonable high transformer core cross sectional area. On the other hand, switching losses due to hard switching would be comparably low, as the blocking voltage is still small. As a compromise, L_M can be chosen large enough to allow soft on-switching starting from a previously determined voltage threshold. This can be done based on the function of the output capacitance C_{oss} over the voltage as shown in Fig. 2, top image. It can be noticed that the output capacitance is increased strongly for voltages less than 100V. As a result, in this design the magnetizing inductance is designed to allow soft switching only when the input voltage is larger than 100V, which occurs for 80% of the time for a sinusoidal input voltage with an amplitude of 325V. From that, the highest allowable magnetizing inductance can be calculated, if a certain maximum switching frequency is fixed (see Fig. 2, second image from top). The overall peak switching frequency for this design is set to $f_{\text{sw,max}} = 800 \text{ kHz}$. This is the highest switching frequency which can be used for attenuation of

a higher input voltage to the desired output voltage of 230V. It has to be stated that the design of the magnetizing inductance is only relevant for the operation point with unity gain, because the resonant converter will then operate at or slightly above resonance frequency. For the operation at higher input voltages, the resonance tank will behave inductive allowing for soft switching either way [3]. This means that the critical peak frequency for determining the magnetizing inductance will be lower than the overall peak frequency of $f_{sw,max} = 800\text{kHz}$ and needs to be calculated by iterating the design loop shown in Fig. 2.

To allow connection to different grid configurations as described before, the resonance converter has to be able to provide a gain of close to one for an input voltage of $U_{in} = 230\text{V}$ and also a gain of close to $A = 0.575$ for an input voltage of $U_{in} = 400\text{V}$. Both operation points have to be available without reconfiguration of the resonance elements, meaning by only adjusting the switching frequency. For this task, generally a design with a high quality factor Q is beneficial, because only smaller frequency variations are required for large changes in the attenuation. Also, it needs to be considered that the quality factor is linearly dependent on the output power. As for the applications aimed for in this paper the load can vary widely, this also can mean an influence on the resonance tank design. As a result, the resonance tank elements L_R and C_R need to be chosen carefully, as shown in Fig. 2, third image from top. For an exemplary minimum power of $P_{min} = 250\text{W}$, the feasible combinations of L_R and C_R as well as the resulting parameters are shown in the table in Fig. 2. The resulting gain plots are shown below. It can be seen that high values of C_R will lead to a lower minimal power requirement and have the possibility of designing a low L_R . On the other hand, low values of C_R can also lead to a sufficiently low minimal power, but will result in overall higher switching frequencies for the operation at unity gain, increasing the losses.

For typical applications, the resonance tank will mostly operate in the area of unity gain. To ensure zero voltage switching for all load conditions, a low magnetizing inductance is necessary. This results in a lower ratio between leakage and magnetizing inductance, consequently, the resonance converter is designed as a LLC converter. This can also lead to a smaller distance between the switching frequency for unity gain and attenuation by $A = 0.575$, allowing for a tighter design in terms of switching losses.

Hardware Prototype

The potential in volume reduction is presented in Fig. 3, were a conventional transformer, a SST with DC storage and the approach shown in this paper are compared. The here proposed solution of a SST without DC storage shows the overall lowest volume which is only 17% of the conventional transformer. The weight is 760g, which is less than 10 % of the reference design. This shows the suitability for weight-sensitive applications like aviation.

The prototype is shown in Fig. 4. All components are mounted on a u-profile heatsink, allowing for a optimal utilization of available space. The PCBs holding the power semiconductors are mounted on the outside of the heatsink arrangement. Additionally, the high frequency stages are mounted on a metal substrate circuit board, which reduces the thermal resistance. This allows the usage of bottom cooled devices, which greatly simplifies the construction. The magnetic components can be mounted in the inside of the heatsink arrangement. The resonance capacitors are directly mounted at the PCB close to the switching node of the half bridges. By minimizing the area, a large parasitic capacitance of the resonance tank against earth can be avoided. This helps in reducing the losses.

As a LLC design is preferred as mentioned before, both the resonance inductor and the transformer can be build up as a single component. The typical ratio of leakage and magnetizing inductance for a LLC lead to a coupling factor of $k = 0.67$ to 0.8 . Such low values can not be reached with conventional winding arrangements, were both windings are wound on the middle core of the ferrite core, even if primary and secondary windings are separated by a special two-chamber coilformer. Instead, a design as shown in Fig. 5, left, is chosen. The primary and secondary windings are located on the outer legs of the core. The middle core is used to control the leakage inductance by adjusting the middle air gap $d_{AG,leak}$. The air gap d_{AG} in the outer legs of the core influences both the leakage and the coupling inductance and is used to realize the desired value of the magnetizing inductance. Consequently, the leakage inductance can

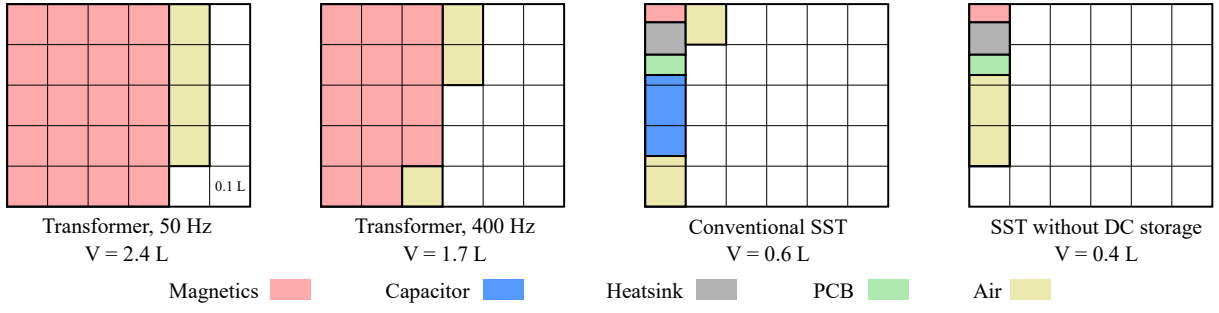


Fig. 3: Volume comparison of conventional transformer for 50 and 400 Hz applications, conventional SST design and SST design without DC storage.

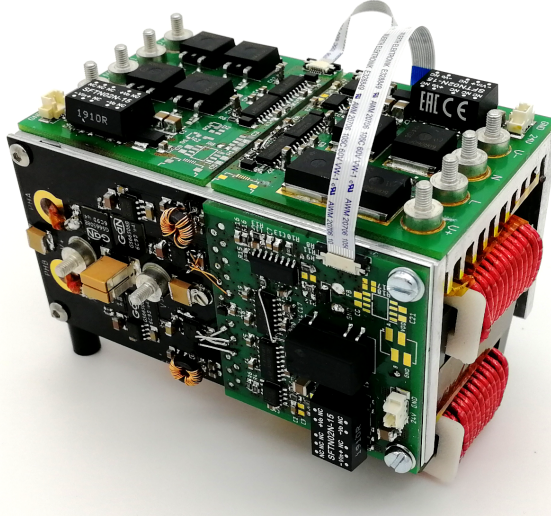


Fig. 4: Design of the SST. All PCBs are mounted on a u-shape heatsink, the magnetic elements are mounted inside. Maximum dimensions are 100 x 58 x 78 mm. Overall weight is 760g.

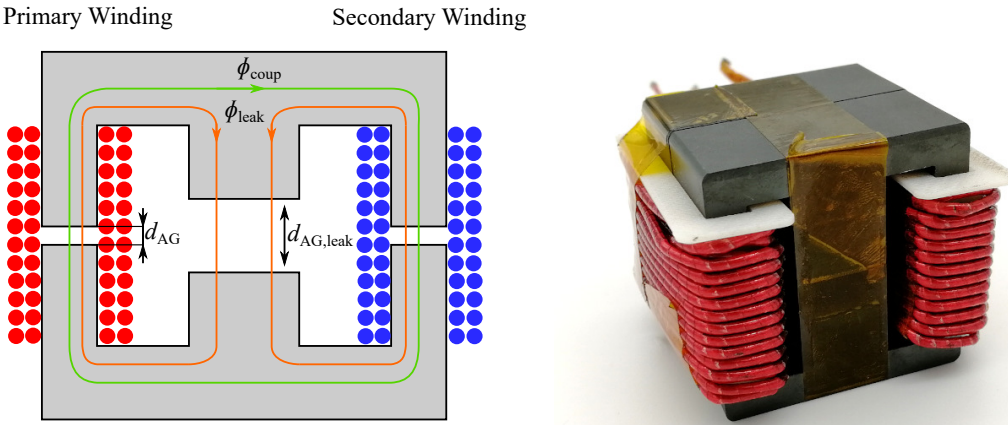


Fig. 5: Design of the integrated resonance inductor and transformer (left), realisation of the design (right).

be designed largely independently from the coupling inductance. Because of that, discrete components of resonance inductor and transformer are not necessary, reducing the overall volume. To accommodate for the reduced core cross sectional area of the outer legs of the ferrite core, two E-cores are stacked in parallel. The resulting dimensions are 43 x 42 x 42 mm³. As both windings are fully separated from each other, the required isolation can be realised. The prototype is shown in Fig. 5, right. The coupling factor was realized as $k = 0.67$.

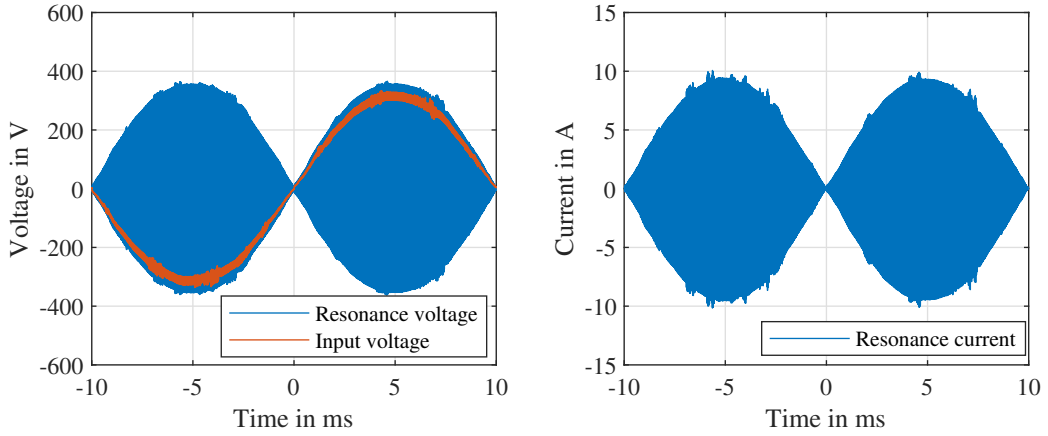


Fig. 6: Waveforms of input voltage and resonance voltage (left) and resonance current (right). Both resonance voltage and current are following the sinusoidal envelope of the rectified input voltage.

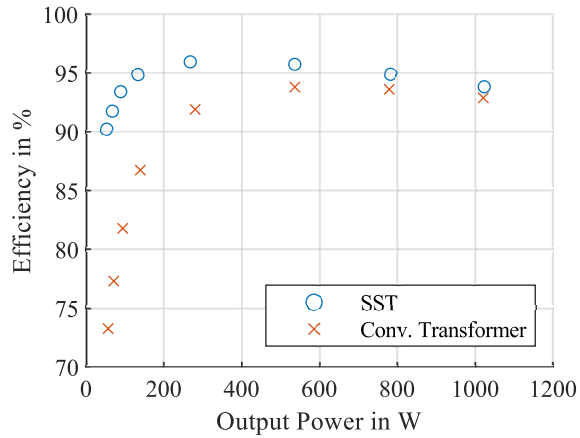


Fig. 7: Comparison of the efficiency of the Solid State Transformer and the reference conventional transformer. The peak efficiency of the SST is 96 %, the efficiency at maximum power is 94 %. The maximum semiconductor temperature at full load was 69.6 °C at the resonance converter fullbridge. The ambient temperature was 26 °C.

To simplify the control, off-the-shelf ICs and analogue control blocks are used. The low frequency fullbridges (S_1 to S_4 and S_{13} to S_{16}) are controlled by a zero-voltage-detection IC, which measures the input voltage. The signal is transferred to the secondary side with a digital isolator. The resonance converter is controlled by an integrated LLC controller. As a feedback to control the output voltage, the voltage at C_2 is rectified and measured. This signal is fed back to the controller by a standard optocoupler circuit. Because no microcontroller is needed, the overall design and PCB layout is simplified.

Measurement Results

For verification of the design, several measurements are conducted. In Fig. 6, the input voltage as well as resonance tank voltage and current are shown. As described before, the input voltage is rectified to sine half waves. This is visible as a sine wave envelope in the resonance voltage and current. The waveforms of input and output voltage and the resulting frequency spectrum obtained by oscilloscope measurement are shown in Fig. 8. As expected, clearly visible peaks at multiples of the switching frequency of the resonance converter are generated. Due to the bipolar modulation, with two half bridges switching at opposing times, the only common mode noise is generated due to slight mismatches of the half bridges at switching [5]. Additionally, the common mode noise is directly coupled back to the noise source via y-capacitors placed close to the switching cells. As a result, only differential mode disturbance contributes

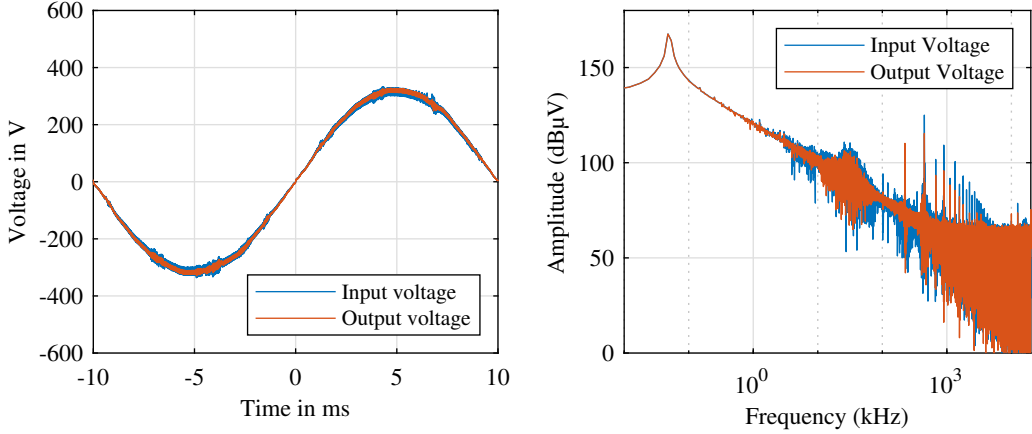


Fig. 8: Waveforms of input and output voltage for operation at unity gain (left) and corresponding frequency spectra (right) obtained by FFT of the oscilloscope measurement data (peak measurement).

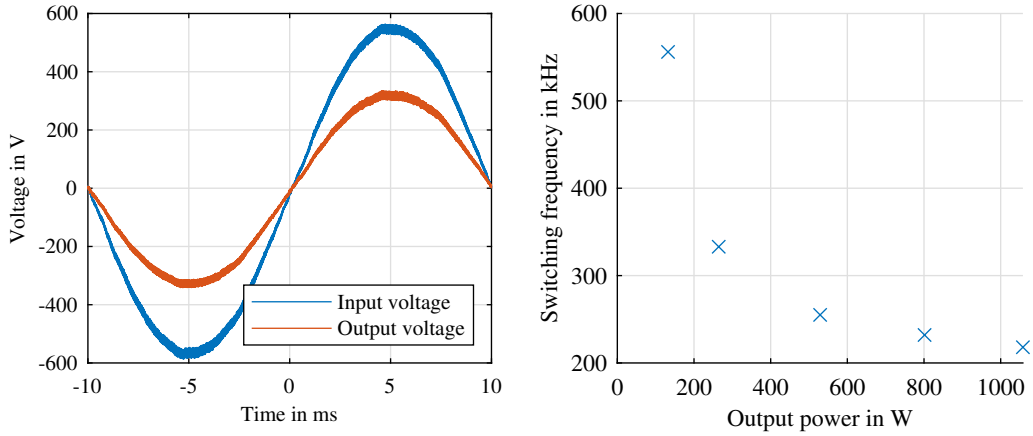


Fig. 9: Stepdown operation from $U_{\text{in}} = 400 \text{ V}$ to $U_{\text{out}} = 230 \text{ V}$. Resulting waveforms for input and output voltages (left) and switching frequency over output power (right). The stepdown operation is possible down to a minimum power of 132 W, which requires a switching frequency of 556 kHz.

to the noise at the input and output of the SST, which can be reduced with little effort by adding small x-capacitors. For the practical application, additional EMI measurements are necessary.

The prototype was operated up to a power of 1 kW. The efficiency in dependency of the output power is shown in Fig. 7. For comparison, also the efficiency of the reference conventional transformer is shown. For all operation points, the efficiency of the SST is higher, with a peak efficiency of 96%. Especially at low power, the losses of the SST are drastically lower, making the application beneficial for applications with varying load and long phases of partial load operation.

Another benefit is the possibility of controlling the output voltage by adapting the gain of the resonance tank. This can be used to stabilize the output voltage during voltage fluctuations of the grid. Also it is possible to provide an output voltage of 230 V for the connection of the SST directly between two phases of the grid, if no neutral point is available. This is shown in Fig. 9, left plot. As stated before, based on the properties of the resonance tank, a certain minimal load is required. With the current design, the step down operation is possible starting from $P_{\text{out}} = 132 \text{ W}$ up to 1 kW, see Fig. 9, right plot. For all loads, switching frequency was below the maximum limit of $f_{\text{sw,max}} = 800 \text{ kHz}$.

Conclusion

Solid state transformer can be a valid alternative to conventional transformers in certain applications. They are beneficial in terms of volume, weight, efficiency and controllability. If the DC storage is

strongly reduced, the input voltage of the resonant converter is comprised of sinusoidal half waves, which can be converted to the secondary side. By that, a pure AC-to-AC converter is gained. While this allows for the reduction of the overall volume, certain points during the design process need to be carefully evaluated. Based on this, a prototype SST with a LLC converter is designed. The magnetic elements are realized as a single component, further reducing the volume. This is achieved by using the outer legs of an E-core for the coupling and modulating the leakage inductance by adapting the air gap in the centre leg. The design is then proven by measurements. An overall peak efficiency of 96% can be realized, which is higher than the efficiency of the conventional design while only having 10% of the weight. Especially at partial load operation, the efficiency is drastically higher compared to the conventional reference transformer. Also, a gain reduction to allow for different operation points was shown. For future research, the proposed solution has to be examined in greater detail in terms of electromagnetic interference. Also, the operation at reactive load needs to be covered in detail.

References

- [1] M. D. Seeman, S. R. Bahl, D. I. Anderson, and G. A. Shah, "Advantages of GaN in a high-voltage resonant LLC converter," in 2014 IEEE Applied Power Electronics Conference and Exposition - APEC 2014, Fort Worth, TX, USA, Mar. 2014 - Mar. 2014, pp. 476–483.
- [2] A. N. Rahman, S.-K. Chen, and H.-J. Chiu, "Single Phase AC-AC Solid State Transformer based on Single Conversion Stage," in 2019 IEEE Workshop on Wide Bandgap Power Devices and Applications in Asia (WiPDA Asia), Taipei, Taiwan, May. 2019 - May. 2019, pp. 1–5.
- [3] H. Wen, J. Gong, C.-S. Yeh, Y. Han, and J. Lai, "An Investigation on Fully Zero-Voltage-Switching Condition for High-Frequency GaN Based LLC Converter in Solid-State-Transformer Application," in 2019 IEEE Applied Power Electronics Conference and Exposition (APEC), Anaheim, CA, USA, Mar. 2019 - Mar. 2019, pp. 797–801.
- [4] K. Tan, R. Yu, S. Guo, and A. Q. Huang, "Optimal design methodology of bidirectional LLC resonant DC/DC converter for solid state transformer application," in IECON 2014 - 40th Annual Conference of the IEEE Industrial Electronics Society, Dallas, TX, USA, Oct. 2014 - Nov. 2014, pp. 1657–1664.
- [5] M. H. Hedayati and V. John, "Filter Configuration and PWM Method For Single-Phase Inverters With Reduced Conducted EMI Noise," IEEE Trans. on Ind. Applicat., vol. 51, no. 4, pp. 3236–3243, 2015, doi: 10.1109/TIA.2014.2387483.